Modulation of TLR Signaling by Multiple MyD88-Interacting Partners Including Leucine-Rich Repeat Fli-I-Interacting Proteins[1]

Penggao Dai,* Sun Yong Jeong,* Yanbao Yu,*†§ Taohua Leng,§ Weidong Wu,‡ Ling Xie,* and Xian Chen[2]*§

Emerging evidences suggest TLR-mediated signaling is tightly regulated by a specific chain of intracellular protein-protein interactions, some of which are yet to be identified. Previously we utilized a dual-tagging quantitative proteomics approach to uncover MyD88 interactions in LPS-stimulated cells and described the function of Fliih, a leucine-rich repeat (LRR) protein that negatively regulates NF-κB activity. Here we characterize two distinct LRR-binding MyD88 interactors, LRRFIP2 and Flap-1, and found that both are positive regulators of NF-κB activity. Upon LPS stimulation, LRRFIP2 was also found to positively regulate cytokine production in macrophages, suggesting a functional role in TLR4-mediated inflammatory response. Furthermore, we observed that immediately following LPS stimulation both LRRFIP2 and Flap-1 compete with Fliih for interacting with MyD88 to activate the signaling. By using a novel multiplex quantitative proteomic approach, we found that at endogenous levels these positive and negative regulators interact with MyD88 in a timely and orderly manner to differentially mediate the NF-κB activity through the course of signaling from initiation to prolongation, and to repression. Based on these data, we describe a mechanistic model in which selective modulation of TLR signaling is achieved by temporal and dynamic interactions of MyD88 with its regulators. *The Journal of Immunology*, 2009, 182: 3450–3460.

Toll-like receptors play a critical role in the innate immune response to infection and disease pathogenesis (1–3). Dysregulated inflammation was shown to correlate with pathological processes such as fibrotic tissue injury and autoimmune diseases such as multiple sclerosis (4–6). Emerging evidence shows that the equilibrium between effective inflammatory response and appropriate cytokine production is tightly and intrinsically regulated by distinct TLR signaling protein complexes involving MyD88 (1). MyD88 is the common intracellular adaptor protein locating immediately downstream of most TLRs; upon TLR stimulation it recruits multiple proteins to precisely control signal transduction (7). During the past few years, a growing number of novel intracellular signal proteins that play either positive or negative roles at multiple levels of TLR-mediated signaling pathways have been individually identified and characterized (1). Recently, much attention has focused on understanding how the immune balance in a mammalian host is achieved (1–3). While most of the characterized regulators of TLRs were found to be working directly through TLR receptors (2, 3, 8), it is thought that other non-TLR-interacting proteins play a regulatory role in controlling TLR signaling. Most importantly, how these positive or negative

regulators cooperate in the same chain of signaling protein-protein interactions is unclear. We reason that the interactions among these signal proteins could be temporally and specifically arranged, contributing to the control of intensity and duration of TLR-mediated signaling for host inflammatory response.

Systems biology approaches, proteomics in particular, provide unique opportunities to identify these agonist-induced multiprotein interactions either in a conserved or temporal fashion (8, 9). In our "unbiased" systems study of the MyD88-interacting signal complex isolated from LPS-stimulated macrophage cells using the newly developed dual-tagging quantitative proteomics approach, we found at least five novel signal proteins previously unknown to interact with MyD88 in a single profiling run (10). The precision and sensitivity of identifying MyD88-specific-interacting partners using our dual-tagging method were ensured by "in-spectra" quantitative markers of amino acid-coded mass tagging (AACT) or stable isotope labeling by amino acids in cell culture (SILAC) (11, 12). Interestingly, following 30 min of LPS stimulation a number of proteins including both categories of leucine-rich repeat (LRR)[3]-containing protein and the LRR-binding proteins were identified as the MyD88-interacting partners in the LPS-stimulated macrophages. The LRR-containing protein Fliih was then characterized as a negative regulator in mediating NF-κB activity functioning through interfering MyD88-TLR4 interaction in an exposure time-dependent manner (10, 13).

In the same profile of LPS-induced MyD88-interacting partners it attracted our attention that there were two distinct LRR- or Fliih-interacting proteins, LRRFIP2 (LRR Fli-I-interacting protein 2)

*Department of Biochemistry and Biophysics, †University of North Carolina-Duke Michael Hooker Proteomics Center, and ‡Department of Pediatrics, Center for Environmental Medicine, Asthma, and Lung Biology, University of North Carolina at Chapel Hill, Chapel Hill, NC 27599; and §Department of Chemistry and Institute of Biomedical Sciences, Fudan University, Shanghai, China

[2] Address correspondence and reprint requests to Dr. Xian Chen, Department of Biochemistry and Biophysics, University of North Carolina at Chapel Hill, Chapel Hill, NC 27599. E-mail address: xian_chen@med.unc.edu

[3] Abbreviations used in this paper: LRR, leucine-rich repeat; Flap-1, Fli-I LRR-associated protein 1, or LRRFIP1; HA, hemagglutinin; iTRAQ, isobaric tag for relative and absolute quantitation; LC-MS/MS, liquid chromatography-mass spectroscopy/mass spectroscopy; LRRFIP2, LRR Fli-I-interacting protein 2; shRNA, short hairpin RNA.

and Flap-1 (Fli-I LRR-associated protein 1, or LRRFIP1), where LRRFIP2 exhibits ~41% sequence homology with the murine Flap-1. Both proteins were originally identified to interact with the LRR domain of human Fliih using the yeast two-hybrid system (14). Recently, Lee and Stallcup reported that Flap-1 directly interacts with β-catenin and activates β-catenin-dependent transcription activity (15). LRRFIP2 interacts with Dvl to increase the cellular levels of β-catenin for activating β-catenin/LEF (lymphocyte enhancer binding factor)/TCF (T cell factor)-dependent transcriptional activity (16). Flap-1 or LRRFIP1 was also shown to bind the TNF-α-308 promoter polymorphism site, suggesting its possible role in the regulation of TNF-α production (17). However, the functional role of LRRFIP2 and Flap-1 in innate immune responses is largely unexplored, although we previously observed by using a luciferase reporter assay that the LRRFIP2 homolog, Flap-1, modestly activates NF-κB (10).

Due to our proteomic finding that both LRR-binding proteins are MyD88-interacting partners, here we characterize the functional role of LRRFIP2 in the LPS-induced TLR4-mediated NF-κB activation and the corresponding cytokine production. We found LRRFIP2 to positively regulate TLR signaling. To reveal the molecular mechanisms underlying how and when the TLR signaling is activated and then shut down through these MyD88-interacting proteins for overall TLR-mediated inflammatory response, without the need for the Ab of each individual interactor, we have also designed an isobaric tag for relative and absolute quantitation (iTRAQ)-based quantitative proteomics (18) approach to measure the TLR agonist-induced binding changes between MyD88 and its multiple partners. We further investigated the correlations between the strength of the interactions of MyD88 with both positive and negative regulators, LRRFIP2, Flap-1, and Fliih, and the activity changes of particular transcription factors at defined time points of agonist exposure. Through our studies using both cell biological and quantitative proteomic approaches, we conclude that the interactions between MyD88 and these two-class regulators that are highly dynamic, and are time course-dependent on the length of cellular exposure to a defined TLR agonist, differentially regulate/modulate the NF-κB activity. Our results directly provided the first systems view about the mechanistic role of TLR agonist-induced temporal interactions among multiple intracellular proteins such as LRRFIP2/Flap-1-MyD88 or Fliih-MyD88 in the selective modulation of TLR signaling.

Materials and Methods

Cell culture and materials

The C3H/HeN-derived macrophage cell line HeNC2 and the C3H/HeJ-derived macrophage cell line GG2EE were kindly provided by Dr. Steven B. Mizel (Wake Forest University, Winston-Salem, NC). The AMJ-C8 cell line stably expressing Flag-calmodulin-binding protein-tagged MyD88 was made by retroviral infection and maintained in DMEM containing 1.8 μg/ml puromycin. The 293T stable cell line expressing Flag-TLR4 was made in the laboratory and maintained in DMEM containing 0.7 μg/ml puromycin, and it was cultured as described previously (13). LPS (from *Escherichia coli* 0111:B4, ultrapure) was purchased from InvivoGen; iTRAQ reagents multiplex kit was a product of Applied Biosystems; anti-FLAG (M2) and anti-hemagglutinin (HA) were from Sigma-Aldrich; and phospho-IκB-α (Ser[32]), IκB-α (44D4), NF-κBp65, phospho-NF-κBp65 (Ser[536]) (93H1) IKKα, and phospho-IKKα/β (Ser[176/180]) (16A6) were from Cell Signaling Technology.

Immunoprecipitation and immunoblotting

The cells were harvested for each condition and lysed with 1$\times$ lysis buffer (1% Nonidet P-40, 50 mM Tris-HCl (pH 7.6), 150 mM NaCl, 2 mM EDTA, 1 mM sodium vanadate, 5 μg/ml leupeptin, 5 μg/ml aprotonin, 1 mM PMSF), then cleared by centrifugation at 12,000 relative centrifugal force. Cell lysates (~400 μg of protein) were incubated without or with

indicated Abs 1 h at 4°C and subsequently with protein A- or protein G-agarose beads overnight at 4°C on a rotating platform. After centrifugation, beads were washed five times with the modified radioimmune precipitation assay buffer. Bound proteins were eluted with the SDS sample buffer, resolved by SDS-PAGE, and transferred onto nitrocellulose membranes (Schleicher & Schuell BioScience). Nitrocellulose membranes were incubated at room temperature for 1 h in blocking buffer containing Tris-buffered saline with 0.1% Tween 20 (TBST) and 5% milk or 5% BSA, followed by incubation with indicated Abs in the blocking buffer. After being washed three times for 5 min each with TBST, the membrane was incubated with HRP-conjugated donkey anti-mouse or anti-rabbit IgG (Amersham Biosciences) followed by washing. Immunoreactive bands were visualized with ECL substrate (Pierce). In some experiments, the nitrocellulose filter was incubated in a buffer containing 62.5 mM Tris-HCl (pH 6.7), 100 mM β-mercaptoethanol, and 2% SDS at 50°C for 30 min and then washed with 0.1% Tween 20 in 50 mM Tris-buffered saline at room temperature for 1 h and reblotted with different Abs. For quantitative analysis, autoradiographic films were scanned with Epson Expression 1680, and the captured image was analyzed with National Institutes of Health Image software.

Luciferase assay

Cells were seeded on 24-well plates 1 day before transfection in 500 μl of growth medium without antibiotics such that they will be 90–95% confluent at the time of transfection. The next day, cells were transfected with 200 ng of pGL2-ELAM promoter luciferase transgene and LRRFIP2/Flap-1 or empty vector plasmid; 20 ng of pRL-TK, which expresses *Renilla* luciferase, was cotransfected as a internal control to normalize the transfection efficiency and sample handling; and 24 h after transfection, the cells were treated with 0.5 μg/ml LPS, 3 μM ODN1826, 25 ng/ml poly(I:C), 10 ng/ml flagellin, and 1 μg/ml ssPolyU for 6 h, and the activities of the two different luciferases were assayed with their respective substrates with a dual luciferase assay kit (Promega). The data presented in the corresponding figures were the normalized NF-κB activity, that is, the values obtained from the division of the firefly luciferase activity by the *Renilla* luciferase activity. The results obtained from triplicated runs of each sample were then averaged. The data presented are the means $\pm$ SE ($n = 3$). Similar results were obtained in three independent experiments.

Expression vectors

Short hairpin RNA (shRNA) expression vectors were generated by the BLOCK-iT lentiviral miR RNA expression system (Invitrogen) according to the manufacturer's instructions. Briefly, LRRFIP2 sequence was analyzed by a program provided by Invitrogen, and three regions were picked and cloned into pENTR/U6 vector to yield pENTR/U6-LRRFIP2[shRNA]. They were cotransfected with a Flag-tagged LRRFIP2 construct into HEK293 cells. Effective clones were identified based on their ability to suppress LRRFIP2 expression by Western blot analysis. The sequences for the pENTR/U6-LRRFIP2[shRNA] constructs is as follows: pENTR/U6-LRRFIP2[shRNA-2], CACCGCAAAGAGATGAGCTTATTGACGAATCAA TAAGCTCATCTCTTTGC.

RNA preparation and real-time PCR

Total RNA was isolated with RNeasy kit (Qiagen). Real-time PCR was performed using SYBR Green as described previously. Primer sequences are available upon request. Results were normalized to GAPDH internal controls and expressed in relative cycle numbers.

Generation of lentiviruses

Sequences encoding pENTR/U6-LRRFIP2[shRNA-2] were inserted into the pLenti6-V5-DEST vector (ViraPower lentiviral expression system; Invitrogen); vectors were transfected together into 293FT cells with the ViraPower packaging mix (Invitrogen) to generate the respective lentiviruses. Viral stocks were made and these were used to infect macrophage cells according to the manufacturer's protocols.

Preparation of human PBMCs

PBMCs were isolated from heparinized peripheral blood from healthy volunteers using Lymphoprep (Nycomed Pharma) and further purified using a discontinuous 31/52% Percoll gradient (Sigma-Aldrich) yielding monocytes of 93% purity, as described previously (19). The remaining cells (7%) of these PBMCs were microscopically identified as lymphocytes with Hema 3 stain. PBMCs were incubated in RPMI 1640 medium containing 10% FBS and 100 μg/ml penicillin/streptomycin at 37°C in 5% CO_2. Cells

were incubated in ultra-low attachment plates (Corning) or polypropylene tubes for LPS stimulation studies.

Transient transfection of primary cells

Transfection of monocytes cells with plasmid DNAs was achieved by electroporation using a Nucleofector and a cell line-specific Nucleofector kit (Amaxa); each electroporation reaction contained 1.5×10^6 cells and 5 μg of plasmid DNA. Transfected cells were plated at a density of 1.5×10^5 cells/well in 24-well plates and incubated for 24 h prior use in experiments. To assess the efficiency of transfection, an aliquot of monocytes cells was transfected with a GFP-expressing vector (pcDNA:hrGFP). Twenty-four hours after transfection, nearly 60% of monocytes cells displayed GFP fluorescence.

iTRAQ labeling of time course-dependent immunoprecipitates

Each aliquot of $\sim 5 \times 10^8$ to 1×10^9 AMJ2-C8 cells expressing FLAG-MyD88 were stimulated with 1 μg/ml TLR7 ligand (R837) for 0, 5, 10, and 30 min, respectively. The cells harvested at each defined time of the agonist exposure was immunoprecipitated with anti-FLAG M2 agarose (Sigma-Aldrich; A2220) following the similar procedure as previously described by Wang et al. (10). Specifically, these cells were lysed in the lysis buffer (50 mM Tris-HCl, 150 mM NaCl, 1% Nonidet P-40) supplemented with PMSF and both protease inhibitor cocktail and phosphatase inhibitor cocktails I and II (Sigma-Aldrich). The soluble fractions were incubated with 250 μl of M2 anti-Flag beads (Sigma-Aldrich) at 4°C for 4 h. The beads were first washed twice with the lysis buffer and then followed by washing twice with $1 \times$ TBS. The immunoprecipitates were eluted by using FLAG peptides (Sigma-Aldrich). For the purpose of iTRAQ labeling of each immunoprecipitate set derived from the cells with each defined length of agonist exposure, a solution containing 100 μg/ml FLAG peptide in $1 \times$ TBS was added in a 5:1 ratio (solution/bead volume) for an overnight incubation with rotation at 4°C. By using Centricon (10 kDa cutoff; Millipore), the eluents were concentrated and the buffer was exchanged with $1 \times$ PBS and then with the iTRAQ dissolution buffer (0.2 M triethylammonium bicarbonate). Alternatively to the elution using FLAG peptides, the immunoprecipitates on the beads could also be eluted with glycin (pH 2.5) and neutralized with 1/20 (v/v) 1 M Tris buffer (pH 8.0). The elutes were then dialyzed against iTRAQ-compatible buffer according to the manufacturer's manual (iTRAQ reagents P/N 4352135; Applied Biosystems). The total protein mass of the eluted immunoprecipitates was quantified by using BCA assay (Pierce) for concurrent tryptic digestion and iTRAQ labeling.

To each sample containing 10–100 μg of eluted immunoprecipitates in 20 μl of the iTRAQ dissolution buffer (0.5 M triethylammonium bicarbonate), 1 μl of the denaturant (2% SDS) and 2 μl of reducing reagent (50 mM Tris(2-carboxyethyl)phosphine)) were added. The sample was then incubated for 1 h at 60°C. One microliter of cysteine-blocking reagent (200 mM methyl methanethiosulfonate in isopropanol) was added and incubated at room temperature for 10 min. The proteins in the immunoprecipitate were digested with trypsin (Promega sequence grade) at a 30:1 protein/enzyme ratio at 37°C overnight. To maximize the iTRAQ labeling efficiency, the total sample volume was kept under 50 μl by using a centrifugal vacuum concentrator. The tryptic peptides from each immunoprecipitate sample were then labeled with each isotope version of the iTRAQ reagents following the manufacturer's instruction (iTRAQ reagents P/N 4352135; Applied Biosystems). In our case the reagent producing a reporter ion at 114 was used for labeling the control sample of nonstimulated cells (0 min), 115 for the cells with 5-min stimulation, 116 for the cell with 10-min stimulation, and 117 for the cells with 30-min stimulation. After iTRAQ labeling, equal amounts (in protein mass) of each of the four peptide samples were mixed and were desalted by using either ZipTip or StageTip (both from Millipore) (19).

MALDI-TOF/TOF liquid chromatography-mass spectroscopy/mass spectroscopy (LC-MS/MS) analysis of iTRAQ-labeled peptide mixtures

The desalted iTRAQ-labeled peptide mixtures were first separated by Tempo nanoflow LC (Applied Biosystems) and the separated peptides were automatically spotted onto a MALDI plate for tandem MS/MS fragmentation on an Applied Biosystems 4800 MALDI-TOF/TOF mass spectrometer. Briefly, each spot was first analyzed in MS mode in the mass range from 800 to 4000 Da by accumulating signal from over 2000 laser shots. Up to 12 parent ions giving MS signals with a signal-to-noise ratio >30 were then selected for further MS/MS fragmentation. The reporter

ions at m/z of 114, 115, 116, and 117 for each peptide sequence were generated for quantitative analysis.

Database search for protein identification and quantitative analysis of time course-dependent changes of MyD88 interactions with signal regulators

All acquired MS/MS spectra were searched against the mouse International Protein Index (IPI) database (version 3.40) using the Mascot (version 2.0; Matrix Science) for peptide sequences and protein identification. Protein-Pilot software (Applied Biosystems) was then used to analyze the relative ratio among the four reporter ions of each peptide. Our focus has been on those peptide signals detected for each individual protein of MyD88, Fliih, LRRPIF2, and Flap-1. First, the peptides identified/sequenced for the corresponding proteins with ion scores >35 (the threshold for highly confident protein identification) were chosen for quantitative analysis. The signal intensity of all unique peptides representing each individual protein with the same iTRAQ tag was measured and averaged. For the peptide signals derived from MyD88, the relative ratio among the four reporter ions corresponding to four time points should be normalized to 1. We first obtained the averaged ratio of 115/114:116/114:117/114 for the MyD88 peptides. The offset percentages for each ratio were obtained when the ratio was normalized to 1. The offset percentages for each ratio were applied to normalize the 115/114:116/114:117/114 ratios of the corresponding peptides of other proteins such as Fliih, LRRPIF2, and Flap-1. The normalized ratios of 115/114, 116/114, and 117/114 for each protein of Fliih, LRRPIF2, and Flap-1 were then used for cross-time point comparisons to determine the effect of time course-dependent agonist stimulation (supplemental Table).[4]

Results

LRRFIP2 and Flap-1 interact with MyD88 in vivo

We first utilized a coimmunoprecipitation method to validate the interaction between LRRFIP2 and MyD88 that was previously identified by our quantitative proteomic approach. Due to the unavailability of the Ab against LRRFIP2, HA-tagged MyD88 and Flag-tagged LRRFIP2/Flap-1 were cotransfected to HEK293T cells. The cell lysates were incubated with HA-conjugated agarose beads to pull down MyD88, and the resulting precipitates were immunoblotted with anti-Flag Ab. As shown in Fig. 1, *A* and *B*, Flag-LRRFIP2 and Flap-1 were all detected in the complexes pulled down against HA-MyD88. To determine how this interaction is regulated by LPS stimulation, the HEK293T cells stably expressing TLR4 were cotransfected with a coreceptor MD2, MyD88, and LRRFIP2 genes and stimulated with 1 μg/ml LPS for different lengths of time after 24-h transfection. Aliquots of the stimulated cells were taken at 5 min, 10 min, 30 min, 1 h, 3 h, and 6 h, respectively, to examine the binding intensity between MyD88 and LRRFIP2. As shown in Fig. 1*C*, in resting cells there was weak binding between these two proteins, and the interaction was strongly enhanced after 5 min of LPS stimulation. Longer LPS exposures showed that the MyD88/LRRFIP2 complex gradually dissociated to basal levels after 6 h of stimulation. The results of quantitative measurements of the strength of these time-resolved interactions are shown in Fig. 1*D*. Through domain truncation analysis, we found that the MyD88-LRRFIP2 interaction requires the N-terminal serine-rich domain, and deletion of this domain prevented LRRFIP2 from interacting with MyD88 (Fig. 1, *A* and *B*).

Both LRRFIP2 and Flap-1 regulate TLR-mediated NF-κB activity and cytokine production in hematopoietic cells

To test whether both LRRFIP2 and Flap-1 were involved in the TLR4 signaling pathway, we used reporter assays to examine the regulatory effects of LRRFIP2 and Flap-1 on NF-κB activity upon

---

[4] The online version of this article contains supplemental material.

FIGURE 1. LRRFIP2 and Flap-1 interact with MyD88 in vivo. *A*, Histogram structures of LRRFIP2 and its truncation mutants. *B*, The interaction of LRRFIP2 and MyD88. HEK293T cells were transfected with 6 μg of HA-MyD88 together with the same amount Flag-Flap-1, Flag-LRRFIP2, Flag-M2, Flag-M5, or Flag-M10 in a 10-cm Petri dish. Cell lysates were incubated with HA-conjugated agarose beads to purify MyD88, and the resulting complex was probed with anti-Flag Ab to show the interaction, and anti-HA Ab to show immunoprecipitation efficiency. Cell lysates were incubated with anti-HA and anti-Flag Ab to show the expression of the constructs. IB indicates immunoblotting; IP, immunoprecipitation; WCL, whole-cell lysates. *C*, LRRFIP2 interaction with MyD88 is regulated by LPS exposure. 293T cells stably expressing TLR4 were transfected with 0.5 μg of MD2, 6 μg of HA-MyD88, and 6 μg of Flag-LRRFIP2; 24 h after transfection, cells were stimulated with 1 μg/ml LPS for varied times as indicated and coimmunoprecipitation was done as in panel *B*. *D*, Quantitative analysis of data in *C*.
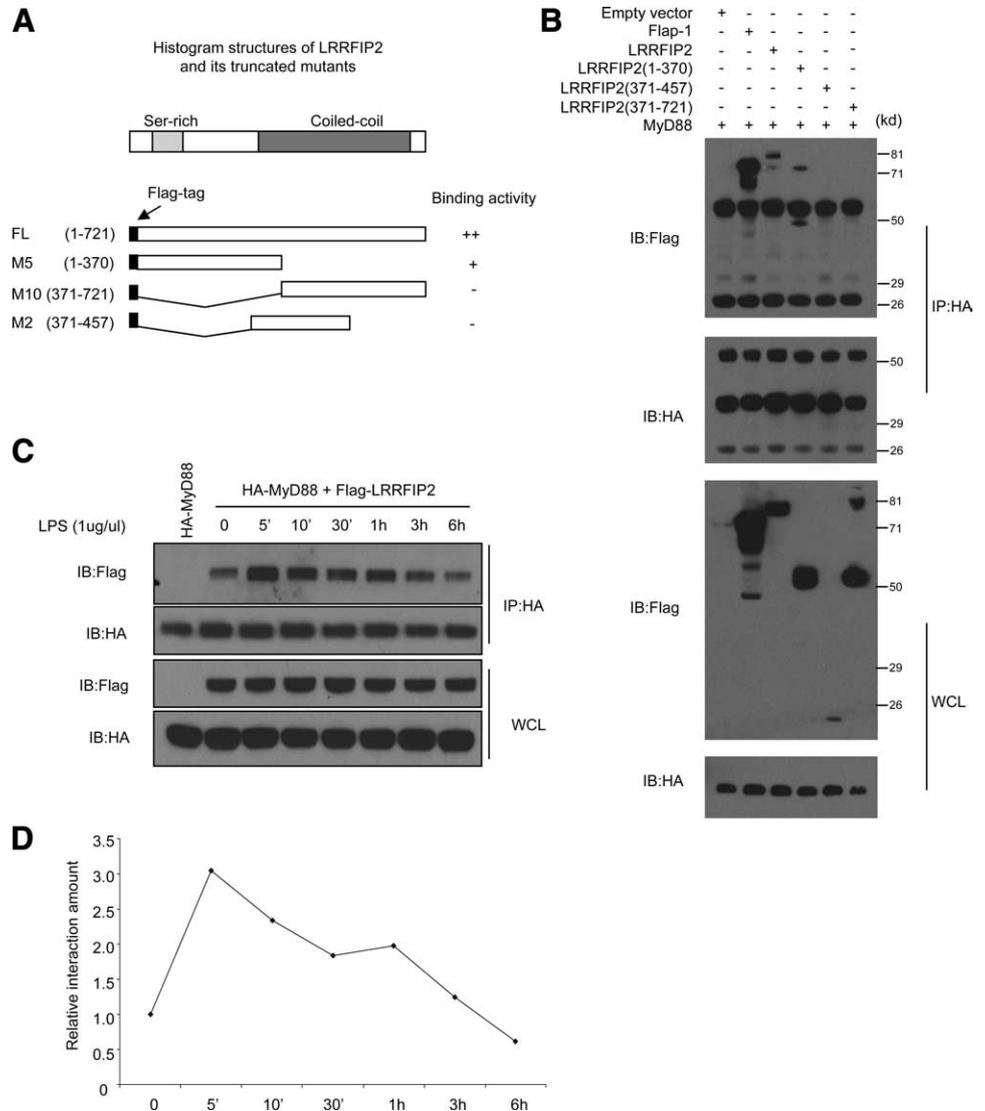
LPS stimulation. We found that both LRRFIP2 and Flap-1 increased the NF-κB promoter activity when overexpressed in RAW264.7 macrophage cells (Fig. 2*A*), and this effect was dose-dependent. Similar effects by LRRFIP2 were seen in HEK293T cells stably expressing TLR4 when cotransfected with a coreceptor MD2 (data not shown). We then confirmed this positive effect by using a 3enh-kB-Con A-luc plasmid as the reporter (20). Similar to its effect on the ELAM reporter gene, LRRFIP2 caused an increase of the Con A promoter activity (Fig. 2*B*).

To determine the role of LRRFIP2 in agonist-induced cytokine production, we comparatively measured the level of TNF-α produced by the LPS-stimulated RAW264.7 macrophage cells transfected with LRRFIP2 or an empty vector as control. As indicated in Fig. 2*C*, the LRRFIP2-transfected macrophages produced more TNF-α than did those from empty vector-transfected macrophages. We also found that LRRFIP2-mediated TNF-α production is LPS-dependent. As shown in Fig. 2*C*, the production of TNF-α was not affected or was slightly affected in the absence of LPS.

We then characterized the effect of LRRFIP2 and Flap-1 on NF-κB activation in primary cells. Human PBMCs isolated from heparinized peripheral blood were transfected with NF-κB reporter gene and the plasmids encoding LRRFIP2 or Flap-1 and luciferase activity was assayed as previously described (21). Compared with

cells transfected with an empty vector, the expression of LRRFIP2 or Flap-1 has increased NF-κB activity for ~5- to 7-fold (Fig. 2*F*). Together with results from RAW264.7 macrophage cells, these observations indicated the positive regulatory role of LRRFIP2 and Flap-1 on NF-κB activation.

To further support this hypothesis, we silenced the endogenous LRRFIP2 expression in THP-1 monocyte cells by using small interfering RNAi. As shown in Fig. 2, *D* and *E*, transfection of HEK293 cells with three constructs of pENTR/U6-LRRFIP2[shRNA-1], -2, and -3 all reduced LRRFIP2 expression by 60%, 90%, and 70%, respectively, compared with a scrambled sequence. The pENTR/U6-LRRFIP2[shRNA-2] shRNAi construct, which had a higher knockdown efficiency, was then used to determine NF-κB activation. In LRRFIP2-silenced THP-1 cells, the NF-κB activity was remarkably decreased compared with that of the control shRNA-transfected cells (Fig. 2*E*).

LRRFIP2 mRNA expression level is regulated by LPS stimulation

In response to agonist-induced activation of host response, many components of signal transduction cascades, including positive and negative regulators, are up-regulated in signaling pathways (22). LRRFIP2 is expressed in multiple tissues, including heart, skeleton
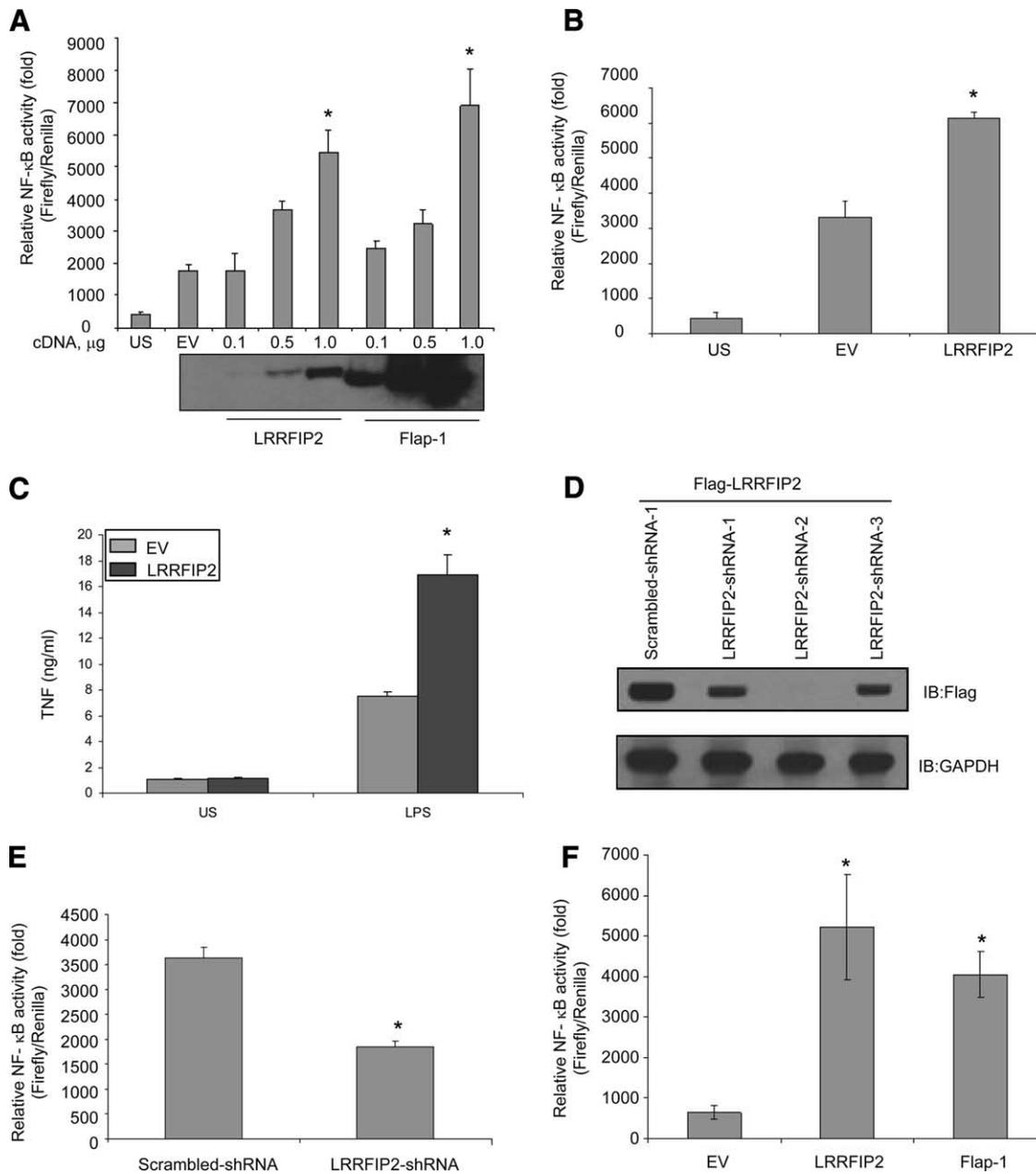
FIGURE 2. Both LRRFIP2 and Flap-1 are activators of the TLR-mediated NF-κB activity in both macrophage cell lines and primary human PBMCs. *A, Top,* Dose-dependent activation of NF-κB in RAW264.7 macrophage cells by LRRFIP2 and Flap-1. RAW264.7 macrophage cells were transfected with NF-κB luciferase reporter gene and various amounts of LRRFIP2/Flap-1 expression constructs or 1 μg of empty control vector (EV) as indicated. Cells were stimulated with 0.5 μg/ml LPS for 6 h or left unstimulated (US) before harvest, and firefly and *Renilla* luciferase activities of the cell lysates were assayed. *Bottom,* Expression of LRRFIP2 and Flap-1. *B,* LRRFIP2 activates the Con 5A luciferase gene. RAW264.7 cells were transfected with pCon 5A luciferase reporter gene, pRL-TK, and 0.4 μg of LRRFIP2 expression constructs; cells were treated as described as panel *A,* and luciferase activities were assayed. *C,* ELISA of TNF-α in culture medium of LRRFIP2 or empty vector (EV) transfected RAW264.7 macrophage cells left untreated or treated for 24 h with LPS (500 ng/ml). *D,* Inhibition of LRRFIP2 expression by LRRFIP2-shRNA constructs. HEK293T cells were cotransfected with 0.4 μg of LRRFIP2 expression constructs and a scrambled 0.4-μg shRNA construct or different LRRFIP2-shRNA constructs, and the resulting cell lysates were analyzed for LRRFIP2 expression 2 days after transfection. *E,* Knockdown of LRRFIP2 suppressed NF-κB activation. THP-1 monocyte cells were transfected with 0.4 μg of LRRFIP2-shRNA constructs or a scrambled construct, NF-κB luciferase gene, and pRL-TK luciferase plasmid, cells were treated as described as *A,* and luciferase activities were assayed. *F,* LRRFIP2 and Flap-1 activation of NF-κB in primary primary human PBMCs. Data represent means ± SEM of triplicate cultures in a single experiment and are representative of two to four experiments. *, *p* < 0.05 for significant differences from control.

muscle, liver, kidney, and pancreas, and it is predominantly expressed in heart and skeletal muscle (14). Due to lack of an Ab against LRRFIP2, we examined the mRNA expression level of endogenous LRRFIP2 in RAW264.7 macrophage cells by RT-PCR and found moderate expression. We then determined the LRRFIP2 expression regulated by LPS stimulation in these cells at various LPS exposure time points. We found that the accumulation of mLRRFIP2 in macrophages significantly increased after 18–24 h LPS exposure as determined by quantitative RT-PCR. We also noticed that the mRNA level of Fliih was altered in response to LPS stimulation (supplemental Fig. 1), suggesting the critical role of LRRFIP2 and Fliih in regulating the activation of TLR4 signaling.

FIGURE 3. Activation of NF-κB through LRRFIP2 is TLR4- and MyD88-dependent. RAW264.7 macrophage cells were transfected with NF-κB luciferase reporter gene and the constructs (0.4 μg) as indicated. Cells were treated and luciferase activity was assayed as in Fig 2, *A* and *B*. HeNC2 and GG2EE macrophage cells were transfected with NF-κB luciferase reporter gene and 0.4 μg of LRRFIP2 construct or control vector. Cells were treated and luciferase activity was assayed as Fig 2*A*. Data represent means ± SEM of triplicate cultures in a single experiment and are representative of two to four experiments. *, $p < 0.05$ for significant differences from control.
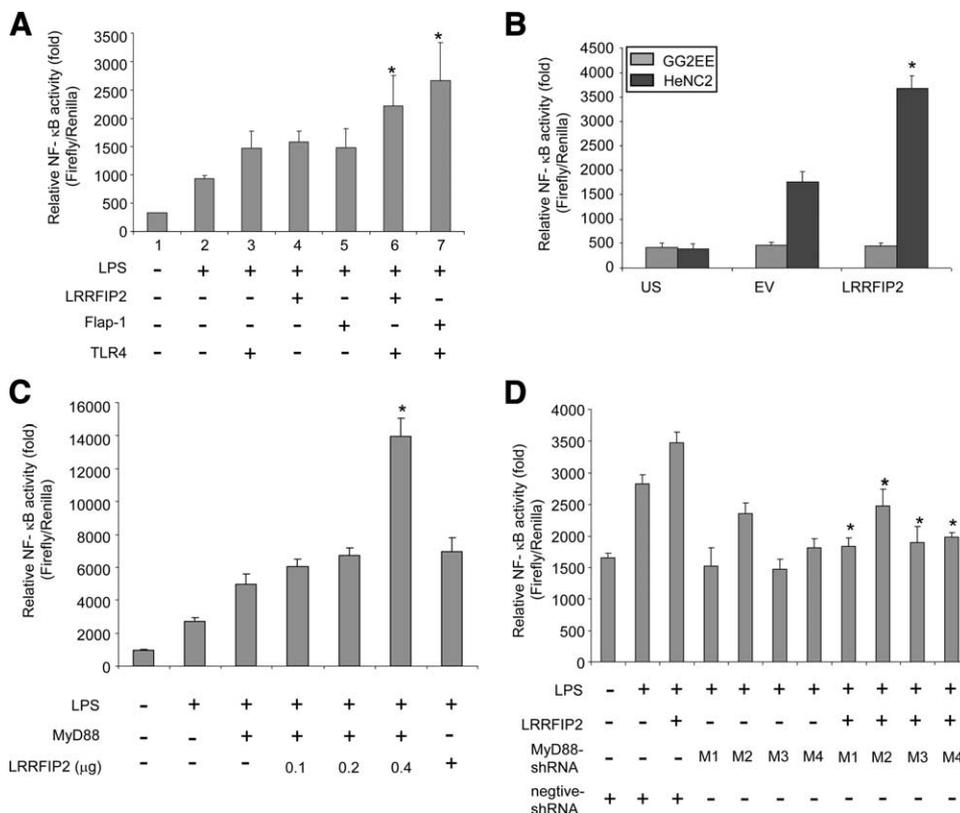
Activation of NF-κB by LRRFIP2 is TLR4-dependent in response to LPS stimulation

We further determined if the NF-κB activation modulated by LRRFIP2 and Flap-1 was mediated by TLR4 in the presence of LPS. RAW264.7 cells was transfected with LRRFIP2, Flap-1, and TLR4 either alone or in a combined manner, respectively, and the NF-κB activity were then measured by reporter assay after 6 h of exposure to LPS. In agreement with an earlier report (23), TLR4 alone induces NF-κB activation. Furthermore, we found that when TLR4 cotransfected with LRRFIP2 or Flap-1, the NF-κB activity was bolstered to a higher level (Fig. 3*A*). This result suggested that TLR4 and LRRFIP2 or Flap-1 worked synergistically to increase NF-κB activity.

To further characterize the direct involvement of TLR4 in the LRRFIP2-modulated NF-κB activation, we took advantage of the available pair of murine macrophage cell lines: HeNC2, or peritoneal macrophages derived from wild-type C3H/HeN mice with functional wild-type TLR4; and GG2EE, or peritoneal macrophages from C3H/HeJ mice lacking functional TLR4 due to a point mutation (24–27). As shown in Fig. 3*B*, HeNC2 exhibited NF-κB activation upon LPS stimulation, whereas no detectable NF-κB activation was found in LPS-treated GG2EE cells. In HeNC2 cells, LRRFIP2 significantly induced NF-κB activation upon LPS stimulation. In contrast, the TLR4-deficient GG2EE cells showed little effect on LRRFIP2-mediated NF-κB activation. These results strongly suggested that LRRFIP2-modulated NF-κB activation is TLR4-dependent.

## Activation of NF-κB by LRRFIP2 is MyD88-dependent in response to LPS stimulation

The adaptor molecule MyD88 is essential for the signaling mediated by most of TLR molecules except for TLR3. To determine whether the NF-κB activation by LRRFIP2 proceeds through either MyD88-dependent or MyD88-independent path-

ways, LRRFIP2 and MyD88 constructs along with the reporter gene were cotransfected into RAW264.7 macrophages and the corresponding NF-κB activity was then assayed. As shown in Fig. 3*C*, cotransfection of LRRFIP2 and MyD88 led to 2-fold increases in NF-κB activity compared with that of the cells transfected with either MyD88 or LRRFIP2 alone.

To further confirm that this positive effect of LRRFIP2 on NF-κB activation is MyD88-dependent, we explored the consequences of MyD88 suppression by using a small interfering RNA approach. In our experimental design four distinct shRNA constructs were chosen to knock down the endogenous MyD88 expression in RAW264.7 macrophage cells, and they have displayed different knockdown efficiency. Among them, the constructs of shRNA-MyD88−1 and -3 were more potent to knock down MyD88 expression (data not shown), as these constructs were transfected into RAW264.7 cells to assay the activity of reporter gene expression. As shown in Fig. 3*D*, shRNA-MyD88-transfected cells had a decreased reporter gene activity. Coexpression of LRRFIP2 did not increase the NF-κB activity, suggesting that LRRFIP2 activation of NF-κB is indeed MyD88-dependent.

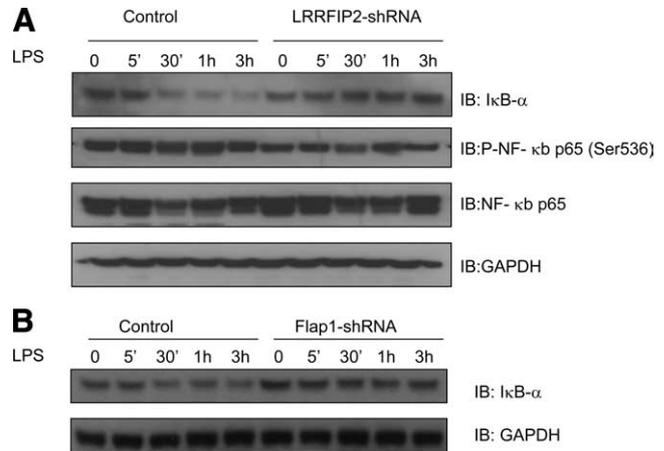## LRRFIP2 activates a variety of distinct TLR signaling pathways

To know if LRRFIP2 can also modulate the activation of other TLR signaling pathways, we treated LRRFIP2-transfected RAW264.7 macrophage cells with different TLR agonists for 6 h and the reporter gene activities were then assayed. LRRFIP2 could modulate the NF-κB activation for all agonists tested (Fig. 4). Among them, LPS (the agonist for TLR4-mediated signaling pathway), poly(I:C) (for TLR3), and ODN1826 (for TLR9) have more pronounced effects on NF-κB activation. Surprisingly, LRRFIP2 also activates the MyD88-independent TLR3 signaling pathway, which utilizes another adaptor protein, Trif. It will be interesting to investigate whether LRRFIP2 interact with Trif to regulate TLR3-mediated signaling pathway.
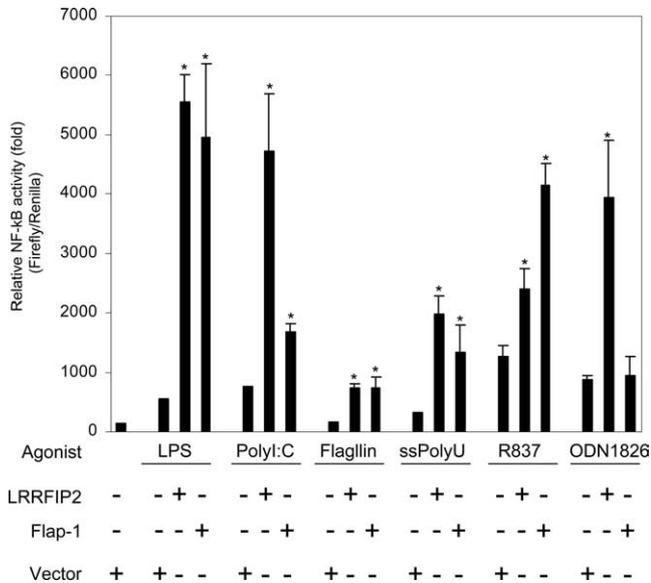
FIGURE 4. Regulation of NF-κB activity through LRRFIP2 and Flap-1 was responsive to different TLR agonists. RAW264.7 macrophage cells were transfected with NF-κB luciferase reporter gene and 0.4 μg of LRRFIP2 or Flap-1 expression constructs as indicated. A *Renilla* luciferase plasmid, pRL-TK, was cotransfected as a control to monitor the transfection efficiency. Twenty-four hours after transfection, the cells were treated with 0.5 μg/ml LPS, 3 μM ODN1826, 25 ng/ml poly(I:C), 10 ng/ml flagellin, and 1 μg/ml ssPolyU for 6 h, and the activities of the two different luciferases were assayed with their respective substrates with a dual luciferase assay kit.


FIGURE 5. Impaired NF-κB signaling in LRRFIP2 and Flap-1 knockdown macrophages. THP-1 monocyte cells were infected by LRRFIP2 shRNA lentivirals (*A*), Flap-1 shRNA lentivirals (*B*), or the control virus (titer 2 × 10^6 transducing U/ml). Forty-eight hours after the transfection, the cells were stimulated with 1 μg/ml LPS for the indicated time. The resulting cells were subjected to analysis of IκB, NF-κB-p65, and p-NF-κB-p65 expression by Western blot. The GAPDH expression level was served as the loading control.

Impaired NF-κB signaling was observed in the LRRFIP2 knockdown macrophages and human PBMCs

LRRFIP2-modulated activation of TLR signaling led us to examine whether the activation state of NF-κB and other key signal proteins such as IκB could be altered in the LRRFIP2-deficient macrophage cells. It is known that the transcription factors NF-κB/Rel are present in the cytosol in an inactive state by complexing with the inhibitory IκB proteins (28, 29). The activation of TLR signaling occurs via phosphorylation of IκB, resulting in the ubiquitin-mediated proteasome-dependent degradation of IκB and the release and nuclear translocation of active NF-κB dimmers, which regulate downstream inflammatory genes (30–32). In our design, THP-1 monocyte cells were infected by LRRFIP2 knockdown lentivirus, which was generated from the LRRFIP2-shRNAi constructs used in Fig. 2. The efficiency of lentivirus silencing was confirmed by real-time RT-PCR to be >75%. First, we examined the activation status of IκB in the LRRFIP2-silenced cells in response to LPS stimulation. The total amount of IκB was observed to be increasing after LPS treatment in the LRRFIP2-deficient cells, reflecting that IκB activation was impaired in the absence of LRRFIP2 protein (Fig. 5). We also examined the NF-κB activation status by detecting phosphorylated NF-κB level. Also as shown in Fig. 5, phosphoryion of NF-κB was inhibited in LRRFIP2-silenced cells, whereas the total NF-κB amount was not significantly changed, as GAPDH was also used to control the loading amount of the total protein. These results suggest a positive role of LRRFIP2 in activation and induction of NF-κB signaling pathway. In further validation of the function of LRRFIP2, primary human monocytes isolated from heparinized peripheral blood were infected by LRRFIP2 knockdown lentivirus as described above. The activation status of IκB and NF-κB were examined after LPS stimulation. As a result we found that the phosphorylation of IκB

was remarkably inhibited in the LRRFIP2-silenced cells in comparison with that of lentivirus-infected cells as control. We observed a similar trend in primary cultured cells (supplemental Fig. 2), which further confirmed the regulatory role of endogenous LRRFIP2 in NF-κB signaling pathway.

Disruption of MyD88-Fliih interaction by LRRFIP2 and Flap-1

We have characterized the individual role of LRRFIP2, Flap-1, and Fliih functioning as either positive or negative regulator(s) in mediating NF-κB activity, respectively. We then investigated the mechanisms by which LRRFIP2 activates the NF-κB pathway, possibly through dynamic interactions among other proteins. The HEK293T cells stably expressing TLR4 were first cotransfected with HA-Fliih, GFP-MyD88, Flag-LRRFIP2, or Flap-1 and MD2. The transfected cells were then treated with either LPS for 5 min or without LPS. The cell lysates then were incubated with HA-conjugated agarose beads to pull down Fliih, and the resulting precipitates were blotted for MyD88 and/or LRRFIP2 and/or Flap-1, respectively. As shown in Fig. 6, Fliih coprecipitated with MyD88 and LRRFIP2 as well as Flap-1. Earlier studies using yeast two-hybrid screening showed that either LRRFIP2 or Flap-1 might be interacting with Fliih (14). Here we provided the similar evidence that LRRFIP2 and Flap-1 each interacts with Fliih in mammalian cells by using a coimmunoprecipitation approach, although no direct evidence showed all of these three proteins were in a same complex all the time through the full course of LPS-induced host response. Interestingly, the existence of LRRFIP2 and Flap-1 greatly disrupted the interaction between Fliih and MyD88 in response to LPS treatment. This suggests that these two proteins act through different mechanisms since the Fliih-interacting abundance of MyD88 was greatly decreased in the presence of LRRFIP2 upon LPS stimulation, but with no significant change in the absence of LPS. Meanwhile Flap-1 constitutively blocked the interaction of Fliih and MyD88 regardless of whether LPS was present. We reasoned that LRRFIP2 and Flap-1 may have a complementary role in regulating the interaction of MyD88 and Fliih. These results demonstrated that LRRFIP2/Flap-1 and Fliih coordinately regulate the signaling transduction.

FIGURE 6. Disruption of the MyD88 and Fliih interaction by Flap-1. HEK293T cells stabling expressing TLR4 were transfected with 4 μg of GFP-MyD88, 4 μg of HA-Fliih, without or with 4 μg of LRRFIP2 or Flap-1. Twenty-four hours after transfection, cells were stimulated without or with 1 μg of LPS for 5 min as indicated. Cell lysates were incubated with HA-conjugated beads to purify Fliih, and the resulting complex was probed with anti-Flag Ab for detection of LRRFIP2 or Flap-1, anti-HA Ab for detection of Fliih, and anti-GFP Ab for detection of MyD88. Expression of transfected proteins was revealed by immunoblotting with the indicated Abs.
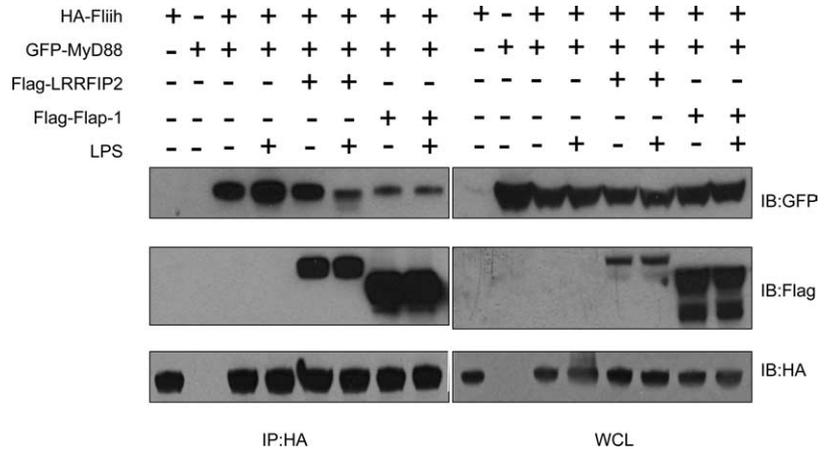
*Quantitation of the dynamic LRRFIP2/Flap-1-MyD88-Fliih interactions using iTRAQ*

We further examined how the endogenous interactions with MyD88 correlate in real time to each responsive stage of stimulated macrophages during the course of MyD88-mediated signal transduction. Here we utilized our newly designed iTRAQ-based quantitative proteomics approach (Y. Sun and X. Chen, manuscript in preparation), which is superior to coimmunoprecipitation-based approaches, which require highly specific Ab for each protein of interest. The iTRAQ approach allows for direct monitoring of the dynamic changes of the interactions with MyD88 at the "snapshot" samples taken from the macrophages at different time points following TLR agonist stimulation (18). Our method measures the agonist-induced simultaneous changes of the MyD88-interacting portion of each signal protein of LRRFIP2 or Flap-1, and Fliih. We used the macrophage cell line AMJ-88, which expresses stably Flag-tagged MyD88 at close to endogenous levels (10). R837, a TLR7 agonist, was used to stimulate the cells due to the higher sensitivity of AMJ-88 in response to R837 than to LPS; its stimulatory effect on the NF-κB activity is similar to that of LPS (Y. Sun and X. Chen, manuscript in preparation). We applied four isobaric tag reagents of an iTRAQ set to label the peptide digests derived from the protein complexes immunoprecipitated by using anti-Flag Ab from the macrophage cells, respectively, collected at 0, 5, 10, and 30 min after R837 stimulation. After equal mixing of the tagged peptide mixtures from these four time points, the
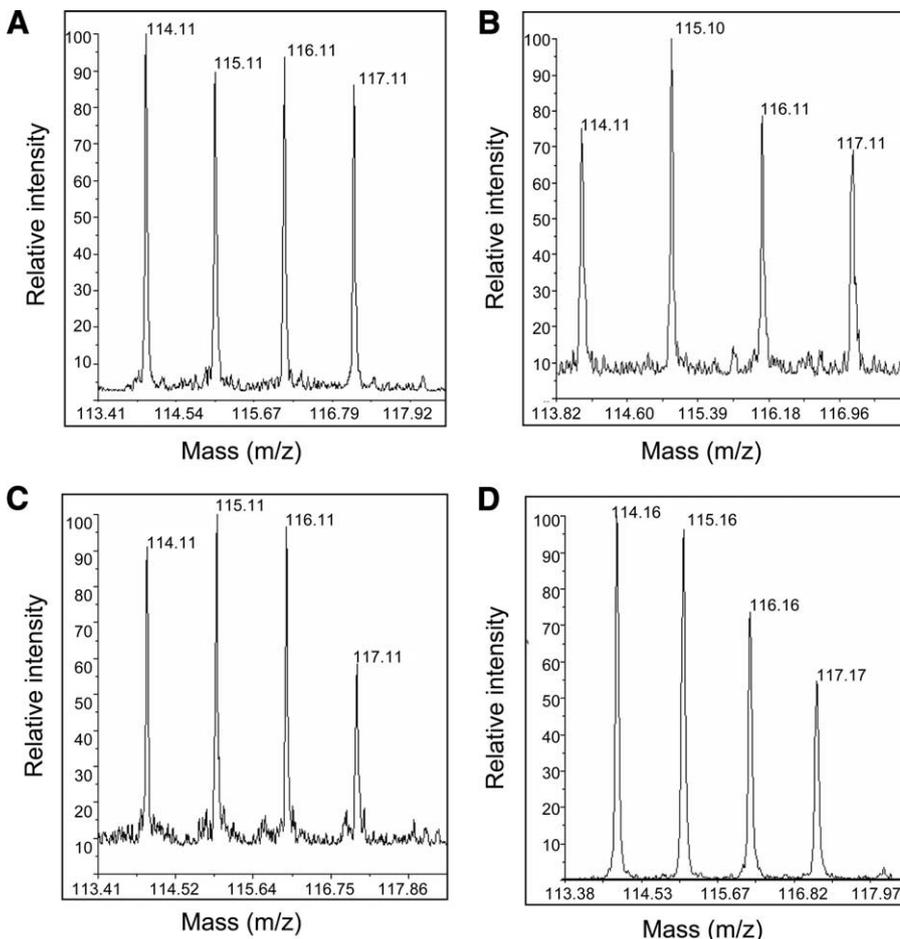
FIGURE 7. The TLR agonist-induced time course-dependent interactions between MyD88 and LRRFIP2 or Fliih monitored by iTRAQ quantitative proteomic approach. The representative mass spectra were derived from (*A*) the peptide LSLFLNPR of MyD88, (*B*) the peptide EELNALK of Flap-1, (*C*) the peptide FSAEDEALSNIAR of LRRFIP2, and (*D*) the peptide VELMPGMR of Fliih. The Flag-tagged MyD88 expressed at close to the endogenous level was used as the bait protein to pull down the complexes at different time points after TLR7 agonist stimulation through immunoprecipitation. The tryptic digests of each time point sample were labeled with each isotope version of the iTRAQ reagent set; that is, the reagent generating reporter ion at *m/z* 114, 115, 116, and 117 was labeling the immunoprecipitates collected from the cells exposed for 0, 5, 10, and 30 min, respectively.

FIGURE 8. Schematic diagram of the switch-on and turn-off mechanism of TLR signaling governed by dynamic and temporal interaction among LRRFIP2, Flap-1, and Fliih in correlation with the full course of signal initiation-propagation-repression. Immediately following TLR agonist stimulation, LRRFIP2, Flap-1, and Fliih are all recruited to interact with MyD88. LRRFIP2 and Flap-1 compete with the negative regulator Fliih for the binding site(s) of MyD88 to initiate the signaling for NF-κB activation. As the signaling progress reaches to certain point (represented here by 60 min), Fliih begins to strengthen its interaction with the TIR domain of TLR molecules to repress the signaling.
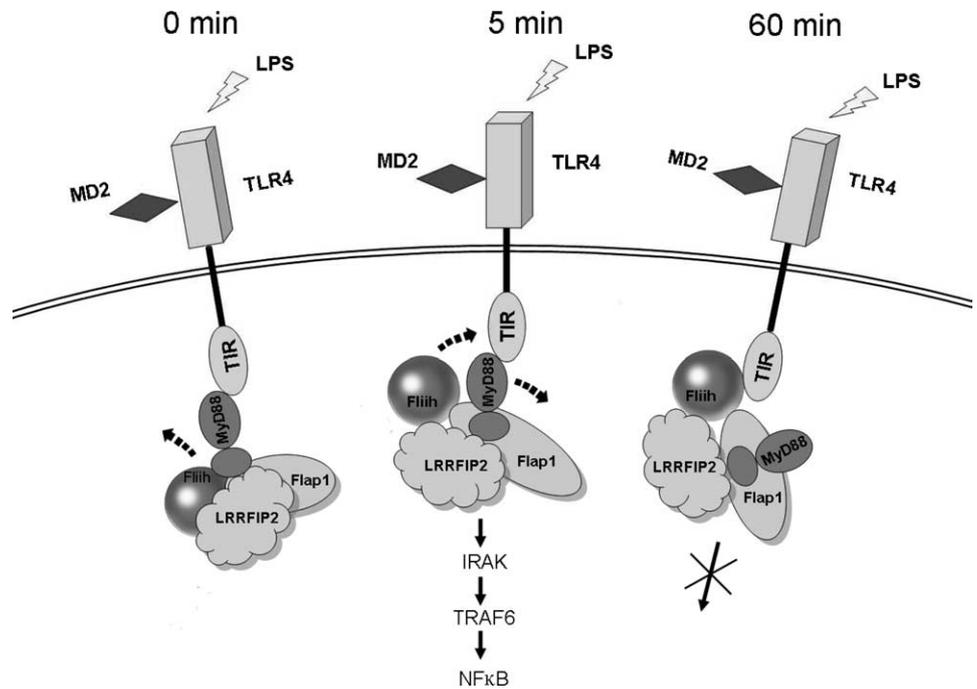
samples were subjected to LC-MS/MS analysis. As shown in Fig. 7, in the set of reporter peptide signals, the *m/z* at 114 Da corresponds to the abundance of a peptide derived from either MyD88 (Fig. 7*A*), Flap-1 (Fig. 7*B*), LRRFIP2 (Fig. 7*C*), or Fliih (Fig. 7*D*) in nonstimulated cells, and the peaks at 115, 116, and 117 Da represent those of MyD88, Flap-1, LRRFIP2, and Fliih peptides originated from the macrophages stimulated for 5, 10, and 30 min, respectively. After the normalization against the MyD88 reporter peptide set, which should theoretically be at unity for all peaks at 114, 115, 116, and 117 Da (Fig. 7*A*), the relative abundance ratios of 115/114:116/114:117/114 for LRRFIP2 and Fliih were at ~1.1: 1.1:0.64 (Fig. 7, *B* and *C*) and 0.90:0.74:0.55 (Fig. 7*D*), respectively. These numbers quantitatively indicated that the interaction of endogenous LRRFIP2 with MyD88 was maximized in 5 min following R837 stimulation, and the MyD88 binding populations of both LRRFIP2 and Flap-1 increased while the MyD88-interacting portion of Fliih was decreased (supplemental Table). With longer times of macrophage exposure to the agonist, the binding trend of all three proteins to MyD88 was reduced. This observation clearly suggested that the temporal and dynamic interactions of key MyD88-interacting proteins correspond to the status of agonist-induced TLR signaling.

Discussion

Regulation of NF-κB activity is a very complex process and is at the crossroad toward either development of appropriate inflammatory response or toward pathological consequences. Thus, its activity must be regulated strictly so that the immune system can be activated to combat pathogen infection without causing any damages in the host. In recent years a number of regulators functioning either positively or negatively in the modulation of NF-κB activity have been individually identified (1). Our unbiased strategy of quantitative proteomics, which is not fully reliant on a pre-convinced notion or hypothesis, has provided a systemic opportunity to simultaneously characterize many additional previously unidentified TLR signaling proteins. Through unbiased proteomic screening, we have previously identified at least 19 MyD88-specific interactions occurring in stimulated living macrophages. Among them, LRRFIP2 and Flap-1, the two structurally and functionally

related and Fliih-LRR-interacting proteins, were previously suggested to play a role in β-catenin/LEF/TCF-dependent transcriptional activation (14, 15). In this study, we present strong evidence for their positive role in regulating TLR-mediated NF-κB activation and cytokine production in macrophages, adding them to the growing list of the TLR signaling regulators. Their regulatory function in TLR signaling was first characterized in macrophage cell lines and later was validated to be consistent at their endogenous level in primary monocytes. Importantly, we found that the actin-binding proteins LRRFIP2, Flap-1 and Fliih (14, 33) have a regulatory role in TLR signaling; this provides the first evidence for the involvement of actin-binding protein in the regulation of TLR signaling.

Together with our previous finding (13), individual signal proteins such as LRRFIP2, Flap-1, and Fliih, all of which interact with MyD88, were found to play an opposing regulatory role in TLR signaling. LRRFIP2 and Flap-1 are closely related proteins associating with the Fliih LRR domain and they showed the similar regulatory role on NF-κB activation. The existence of two MyD88-interacting proteins with similar structure and function raised several questions. What is the differential role for their interactions with MyD88 or Fliih in modulating NF-κB activity? Do they interact competitively or cooperatively for regulating TLR signaling?

Through the combined results from both biological characterization and the real-time quantitative proteomic approach, we have further shown that the length of host exposure to a TLR agonist determines the interactivity and the relative binding strength among LRRFIP2/Fliih/MyD88. First, the interaction between MyD88 and LRRFIP2 reached to a maximum level at 5–10 min of LPS stimulation. These two proteins then gradually disassociated upon further stimulation. Second, addition of LRRFIP2 and Flap-1 competitively disrupt the interaction between MyD88 and Fliih at an early stage of TLR agonist stimulation. While it is important to shut down the overactivation of NF-κB for cytokine production, the immune system needs to achieve a proper activation level when the signaling is overinhibited. In this regard, LRRFIP2/ Flap-1 competitively disrupt the interaction of MyD88 and Fliih

during agonist-induced signal transduction, thus temporally releasing the negative regulation of TLR signaling to keep a proper activation level. As our results also indicated that LRRFIP2 disruption of MyD88-Fliih interaction requires LPS stimulation, whereas Flap-1 constitutively disrupts the MyD88-Fliih interaction, we speculate that Flap-1 may serve as a primary inducer of TLR signaling when the invading agonist is at low level. In certain circumstances, Flap-1 alone may not be sufficient to activate the signaling, and then LRRFIP2 interacts with Fliih, leading to further releasing of the negative regulators and thus fully activating the signaling pathway.

So far, for unknown reasons, most negative regulators seem to target the MyD88-dependent pathway, with the notable exceptions of Fliih, A20, and TRAILR, which also target the MyD88-independent pathway (13, 34, 35). LRRFIP2 and Flap-1 activate several TLR signaling pathway upon stimulation by different agonists, suggesting that they target both the MyD88-dependent and MyD88-independent pathways. It will be interesting to determine whether LRRFIP2 and Flap-1 also interact with the adaptor protein Trif, which is used by the MyD88-independent pathway.

We also noticed that LRRFIP2 is a serine-rich protein, and in our LC-MS/MS studies of LRRFIP2 a total of 1 threonine and 19 serine phosphorylation sites were identified (our unpublished results). This result implies that the possible agonist-stimulated phosphorylations on LRRFIP2 may play an important role in regulating its interactions with other proteins. The functional roles of these phosphorylation sites are under investigation and will be reported elsewhere.

As depicted in Fig. 8, based on our results of systems investigation using both cell biological and proteomic approaches, we propose a mechanistic model elucidating how the differential regulation for modulating TLR-mediated signaling is achieved through well-defined temporal and dynamic interactions among our newly characterized MyD88-interacting proteins. Although this model is postulated partially based on a TLR7 agonist-stimulated profile of dynamic interactions, it may also apply to TLR4-mediated signaling. We speculate that LRRFIP2 and Flap-1 compete with Fliih at the same binding site at MyD88. In resting cells, Flap-1 constitutively interacts with both MyD88 and Fliih. Following LPS stimulation, more LRRFIP2s were recruited to the MyD88-interacting complex, meanwhile competitively weakening/disrupting the interaction between MyD88 and Fliih. The temporal release of the negative regulator in signaling, Fliih, from its association with MyD88, which remains interacting with the TIR (Toll/IL-1 receptor) domain of TLR4 molecules, elevates the NF-κB activity to a proper level. During signaling, excess Fliih disassociates from the MyD88 complex and starts to compete with MyD88 for the TIR domain of TLR4 and to destabilize the MyD88-TLR4 complex. The pronounced interaction between Fliih and TIR leads to reduction of NF-κB activity. As a result, these time course-dependent cooperative interactions among LRRFIP2, Flap-1, Fliih, and MyD88 induced by particular TLR agonists govern the intensity and duration of TLR-mediated inflammatory responses.

In summary, our design combining an unbiased phenotype-specific proteomic screening with concurrent biological characterization of dynamic interactions of multiple signal proteins clearly demonstrated the strength of systems investigation in dissecting the complexity of signal modulation. Following the characterization of their diverse regulatory roles in TLR signaling of individual signal proteins, we further illustrated how the dynamic interactions of multiple signal proteins at MyD88 level, which closely correlate with the length of agonist stimulation, modulate either synergistically or differentially the strength and duration of NF-κB activa-

tion. These observations suggests an elegant signal "switch-on" and "turn-off" mechanism that depends on the temporal and dynamic nature of specific protein-protein interactions to prevent the host system from being either "overinhibited" or "over-heated", that is, to ensure that the sufficient level of inflammatory response can be induced to combat pathogens and that the positive regulators, such as LRRFIP2/Flap-1, can strengthen their interactions with MyD88 to maintain a proper activation level when the signaling is overinhibited. Meanwhile, once sufficient cytokine production has been achieved, the negative regulators such as Fliih dominate the interaction with the TIR domain of TLR4 to avoid overheating the system. Furthermore, these signal proteins, such as LRRFIP2, Flap-1, or Fliih, which mediate either induction or repression of TLR signaling, together serve as a signal balance in coordinating inflammatory response after infection, and they may be a novel target in the control of agonist-induced TLR-mediated inflammatory and autoimmune diseases.

Disclosures

The authors have no financial conflicts of interest.

References

1. Liew, F. Y., D. Xu, E. K. Brint, and L. A. O'Neill. 2005. Negative regulation of Toll-like receptor-mediated immune responses. *Nat. Rev. Immunol.* 5: 446–458.
2. Dunne, A., and L. A. O'Neill. 2003. The interleukin-1 receptor/Toll-like receptor superfamily: signal transduction during inflammation and host defense. *Sci. STKE* 2003: re3.
3. Janeway, C. A., Jr., and R. Medzhitov. 2002. Innate immune recognition. *Annu. Rev. Immunol.* 20: 197–216.
4. Akira, S., and K. Takeda. 2004. Toll-like receptor signalling. *Nat. Rev. Immunol.* 4: 499–511.
5. Medzhitov, R. 2001. Toll-like receptors and innate immunity. *Nat. Rev. Immunol.* 1: 135–145.
6. Takeda, K., T. Kaisho, and S. Akira. 2003. Toll-like receptors. *Annu. Rev. Immunol.* 21: 335–376.
7. O'Neill, L. A. 2003. The role of MyD88-like adapters in Toll-like receptor signal transduction. *Biochem. Soc. Trans.* 31: 643–647.
8. Blagoev, B., I. Kratchmarova, S. E. Ong, M. Nielsen, L. J. Foster, and M. Mann. 2003. A proteomics strategy to elucidate functional protein-protein interactions applied to EGF signaling. *Nat. Biotechnol.* 21: 315–318.
9. Bouwmeester, T., A. Bauch, H. Ruffner, P. O. Angrand, G. Bergamini, K. Croughton, C. Cruciat, D. Eberhard, J. Gagneur, S. Ghidelli, et al. 2004. A physical and functional map of the human TNF-α/NF-κB signal transduction pathway. *Nat. Cell. Biol.* 6: 97–105.
10. Wang, T., S. Gu, T. Ronni, Y. C. Du, and X. Chen. 2005. In vivo dual-tagging proteomic approach in studying signaling pathways in immune response. *J. Proteome Res.* 4: 941–949.
11. Chen, X., L. M. Smith, and E. M. Bradbury. 2000. Site-specific mass tagging with stable isotopes in proteins for accurate and efficient protein identification. *Anal. Chem.* 72: 1134–1143.
12. Ong, S. E., B. Blagoev, I. Kratchmarova, D. B. Kristensen, H. Steen, A. Pandey, and M. Mann. 2002. Stable isotope labeling by amino acids in cell culture, SILAC, as a simple and accurate approach to expression proteomics. *Mol. Cell. Proteomics* 1: 376–386.
13. Wang, T., T. H. Chuang, T. Ronni, S. Gu, Y. C. Du, H. Cai, H. Q. Sun, H. L. Yin, and X. Chen. 2006. Flightless I homolog negatively modulates the TLR pathway. *J. Immunol.* 176: 1355–1362.
14. Fong, K. S., and H. G. de Couet. 1999. Novel proteins interacting with the leucine-rich repeat domain of human flightless-I identified by the yeast two-hybrid system. *Genomics* 58: 146–157.
15. Lee, Y. H., and M. R. Stallcup. 2006. Interplay of Fli-I and FLAP1 for regulation of β-catenin dependent transcription. *Nucleic Acids Res.* 34: 5052–5059.
16. Liu, J., A. G. Bang, C. Kintner, A. P. Orth, S. K. Chanda, S. Ding, and P. G. Schultz. 2005. Identification of the Wnt signaling activator leucine-rich repeat in Flightless interaction protein 2 by a genome-wide functional analysis. *Proc. Natl. Acad. Sci. USA* 102: 1927–1932.
17. Suriano, A. R., A. N. Sanford, N. Kim, M. Oh, S. Kennedy, M. J. Henderson, K. Dietzmann, and K. E. Sullivan. 2005. GCF2/LRRFIP1 represses tumor necrosis factor alpha expression. *Mol. Cell. Biol.* 25: 9073–9081.
18. Zieske, L. R. 2006. A perspective on the use of iTRAQ reagent technology for protein complex and profiling studies. *J. Exp. Bot.* 57: 1501–1508.
19. Soukup, J. M., and S. Becker. 2003. Role of monocytes and eosinophils in human respiratory syncytial virus infection in vitro. *Clin. Immunol.* 107: 178–185.

20. Gil, J., and M. Esteban. 2000. The interferon-induced protein kinase (PKR), triggers apoptosis through FADD-mediated activation of caspase 8 in a manner independent of Fas and TNF-α receptors. *Oncogene* 19: 3665–3674.

21. Dai, P., W. C. Xiong, and L. Mei. 2006. Erbin inhibits RAF activation by disrupting the sur-8-Ras-Raf complex. *J. Biol. Chem.* 281: 927–933.

22. McDonald, C., F. F. Chen, V. Ollendorff, Y. Ogura, S. Marchetto, P. Lecine, J. P. Borg, and G. Nunez. 2005. A role for Erbin in the regulation of Nod2-dependent NF-κB signaling. *J. Biol. Chem.* 280: 40301–40309.

23. Beutler, B. 2000. Tlr4: central component of the sole mammalian LPS sensor. *Curr. Opin. Immunol.* 12: 20–26.

24. Qureshi, S. T., L. Lariviere, G. Leveque, S. Clermont, K. J. Moore, P. Gros, and D. Malo. 1999. Endotoxin-tolerant mice have mutations in Toll-like receptor 4 (Tlr4). *J. Exp. Med.* 189:615–625.

25. Poltorak, A., X. He, I. Smirnova, M. Y. Liu, C. Van Huffel, X. Du, D. Birdwell, E. Alejos, M. Silva, C. Galanos, et al. 1998. Defective LPS signaling in C3H/HeJ and C57BL/10ScCr mice: mutations in *Tlr4* gene. *Science* 282: 2085–2088.

26. Lehner, M. D., S. Morath, K. S. Michelsen, R. R. Schumann, and T. Hartung. 2001. Induction of cross-tolerance by lipopolysaccharide and highly purified lipoteichoic acid via different Toll-like receptors independent of paracrine mediators. *J. Immunol.* 166: 5161–5167.

27. Hoshino, K., O. Takeuchi, T. Kawai, H. Sanjo, T. Ogawa, Y. Takeda, K. Takeda, and S. Akira. 1999. Cutting edge: Toll-like receptor 4 (TLR4)-deficient mice are hyporesponsive to lipopolysaccharide: evidence for TLR4 as the *Lps* gene product. *J. Immunol.* 162:3749–3752.

28. Verma, I. M., J. K. Stevenson, E. M. Schwarz, D. Van Antwerp, and S. Miyamoto. 1995. Rel/NF-κB/IκB family: intimate tales of association and dissociation. *Genes Dev.* 9: 2723–2735.

29. Baldwin, A. S., Jr. 1996. The NF-κB and IκB proteins: new discoveries and insights. *Annu. Rev. Immunol.* 14: 649–683.

30. Yamamoto, Y., and R. B. Gaynor. 2004. IκB kinases: key regulators of the NF-κB pathway. *Trends Biochem. Sci.* 29: 72–79.

31. Viatour, P., M. P. Merville, V. Bours, and A. Chariot. 2005. Phosphorylation of NF-κB and IκB proteins: implications in cancer and inflammation. *Trends Biochem. Sci.* 30: 43–52.

32. Ghosh, S., and M. Karin. 2002. Missing pieces in the NF-κB puzzle. *Cell* 109(Suppl.): S81–S96.

33. Archer, S. K., C. A. Behm, C. Claudianos, and H. D. Campbell. 2004. The flightless I protein and the gelsolin family in nuclear hormone receptor-mediated signalling. *Biochem. Soc. Trans.* 32: 940–942.

34. Diehl, G. E., H. H. Yue, K. Hsieh, A. A. Kuang, M. Ho, L. A. Morici, L. L. Lenz, D. Cado, L. W. Riley, and A. Winoto. 2004. TRAIL-R as a negative regulator of innate immune cell responses. *Immunity* 21: 877–889.

35. Boone, D. L., E. E. Turer, E. G. Lee, R. C. Ahmad, M. T. Wheeler, C. Tsui, P. Hurley, M. Chien, S. Chai, O. Hitotsumatsu, et al. 2004. The ubiquitin-modifying enzyme A20 is required for termination of Toll-like receptor responses. *Nat. Immunol.* 5: 1052–1060.